Supporting Information

3D-Printed Mesoporous-Silica-Confined Perovskite Quantum Dot Micro-Optics for Geometry-Tailored Color Conversion in Micro-LED Displays

Chuyu Qin, Mengyang Wang, Aixin Luo, Guangda Du, Jiaxian Liu, Zekai Hong, Tingshi Yang, Pu Zhang, Chunlin Ma, Luyu Cao*, Yayun Zhou*, Bingfeng Fan*

Guangdong-Hong Kong-Macao Joint Laboratory for Intelligent Micro-Nano Optoelectronic Technology, School of Physics and Optoelectronic Engineering, Foshan University, Foshan, 528225, China

*E-mail: caoluyu@fosu.edu.cn (L. Y. Cao), zhouyayun@fosu.edu.cn (Y. Y. Zhou), binzsu@163.com (B. F. Fan)

Characterization

The X-ray diffraction (XRD) patterns were identified by the laboratory powder X-ray diffraction system (D8 DISCOVER) at a scanning rate of 10° per minute in the 2θ range from 10° to 70°. The morphology and element mapping of the as-prepared products were inspected using scanning transmission electron microscopy (STEM, Talos F200X G2). Time-resolved decay, Excitation and emission spectra were recorded by a fluorescence spectrometer (Edinburgh Instruments FLS1000). High-resolution transmission electron microscope (HRTEM) and electron diffraction patterns were acquired using a Tecnai G2 F30. N_2 adsorption/desorption isotherms of MSNs were obtained by using a gas adsorption analyzer (ASAP 2460). The internal and external quantum efficiencies (η_{IQE} and η_{EQE}) were measured using a fluorescence spectrometer equipped with an integrating sphere (Hamamatsu Photonics, Quantaurus-QY C11347). Operationally, we firstly record the blank (quartz cell) under 365 nm excitation, then record the sample under identical conditions; the instrument integrates the sample emission over 300-950 nm and computes η_{EQE} from the difference in reflected excitation between blank and sample according to the above equation. Therefore, the "IQE" we report is numerically the absolute photoluminescence quantum yield (absolute PLQY) of the powder obtained by the integrating-sphere method. η_{IQE} and η_{EQE} were calculated based on the following equation:

$$\eta_{IQE} = \frac{\int L_S}{\int E_R - \int E_S} \quad \text{(S1)}$$

$$\eta_{EQE} = \frac{\int L_S}{\int E_R} \quad \text{(S2)}$$

where L_S stands for the emissive photons of the sample, E_R and E_S are the reflected photons of excitation light with the blank reference and sample, respectively.

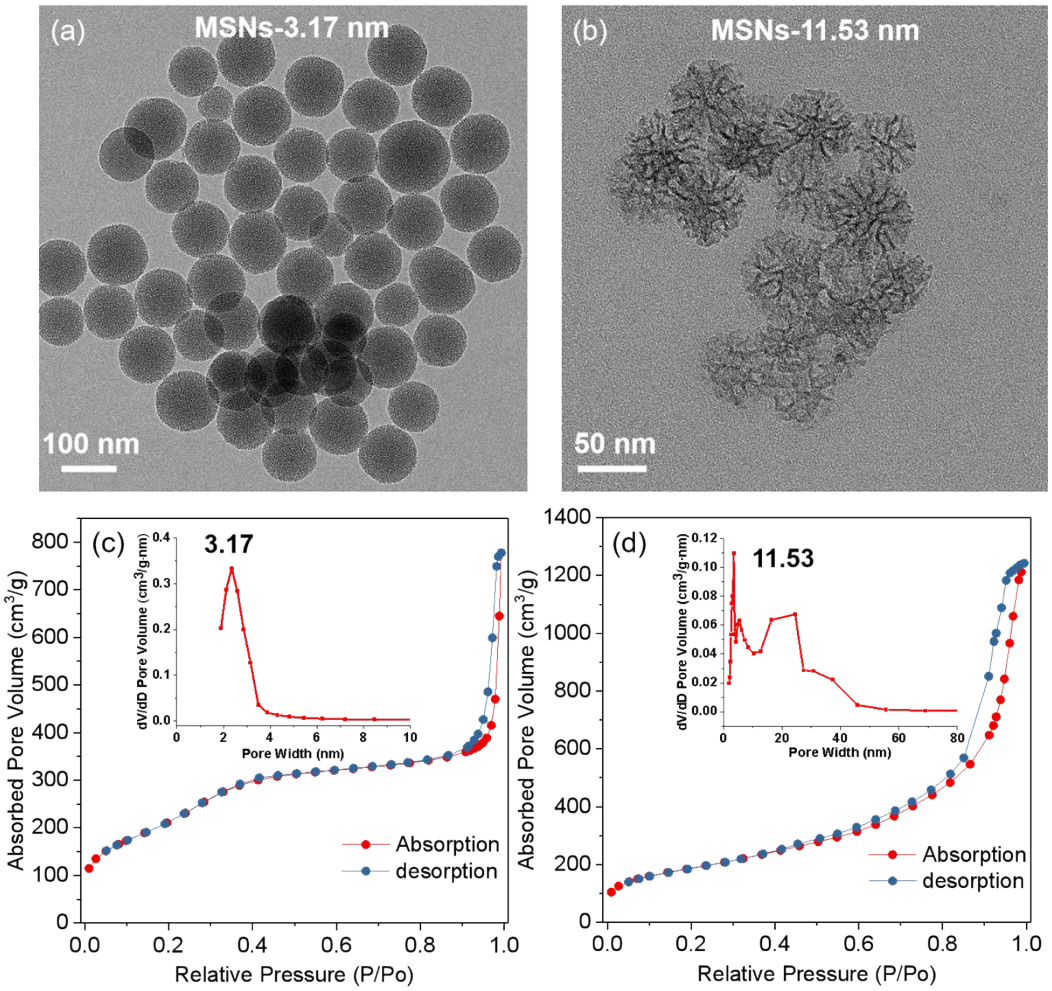

Figure S1. TEM images of (a) MSNs-3.17 nm and MSNs-11.53 nm. N_2 adsorption/desorption isotherm and pore size distributions (inset) of (c) MSNs-3.17 nm and (d) MSNs-11.53 nm.

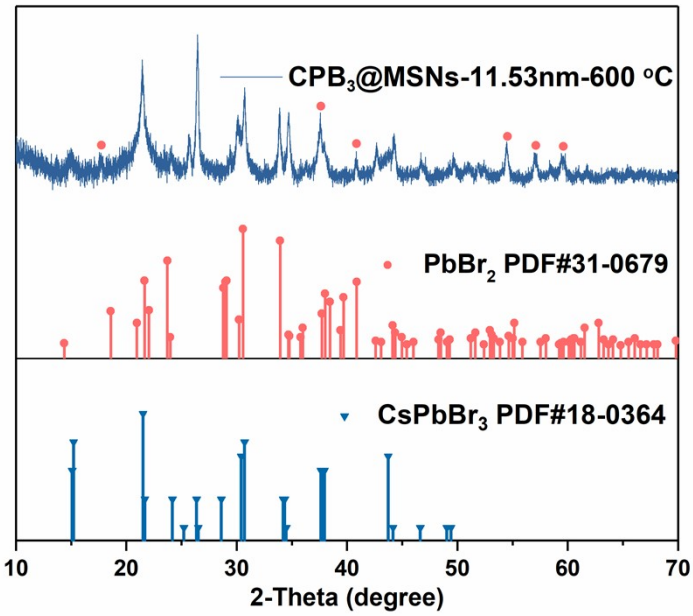

Figure S2. XRD pattern of CPB@MSNs-11.53 nm (annealing temperature: 600 °C) and the standard pattern for $PbBr_2$ (JCPDS No.31-0679) and $CsPbBr_3$ (JCPDS No.18-0364).

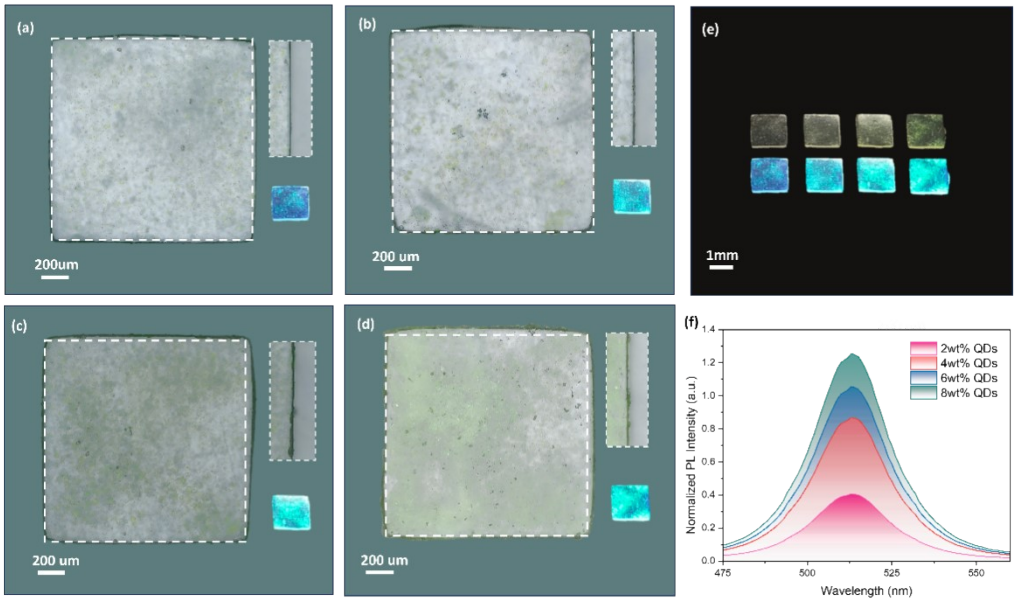

Figure S3. (a–d) Optical microscopy images of printed QD-containing thin films with QD loadings of 2, 4, 6, and 8 wt%, respectively. The dashed squares indicate the designed printing area; the insets show the edge region and the corresponding emission under 405 nm excitation. (e) Photographs of printed patterns with increasing QD loading (2–8 wt%, left to right) under ambient light (top) and UV irradiation (bottom). (f) Normalized photoluminescence (PL) spectra of the thin films at different QD loadings. Scale bars: 200 μm in (a–d) and 1 mm in (e).

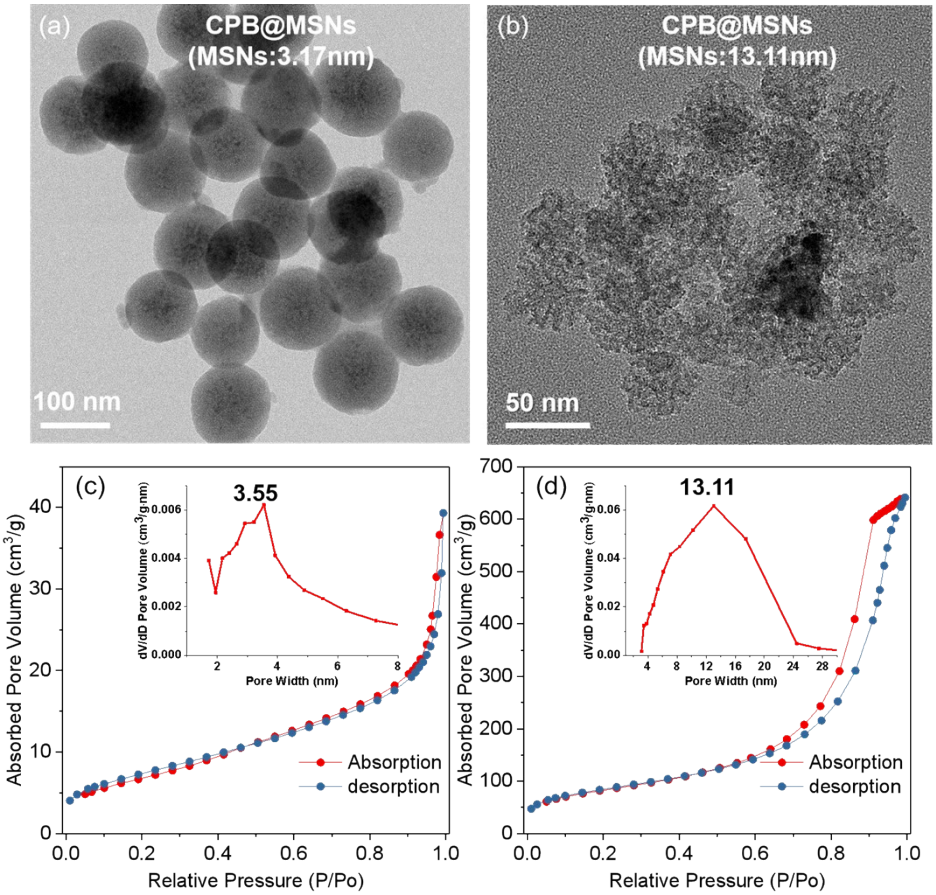

Figure S4. TEM images of (a) CPB@MSNs-3.17 nm and CPB@MSNs-11.53 nm. N_2 adsorption/desorption isotherm and pore size distributions (inset) of (c) CPB@MSNs-3.17 nm and (d) CPB@MSNs-11.53 nm.

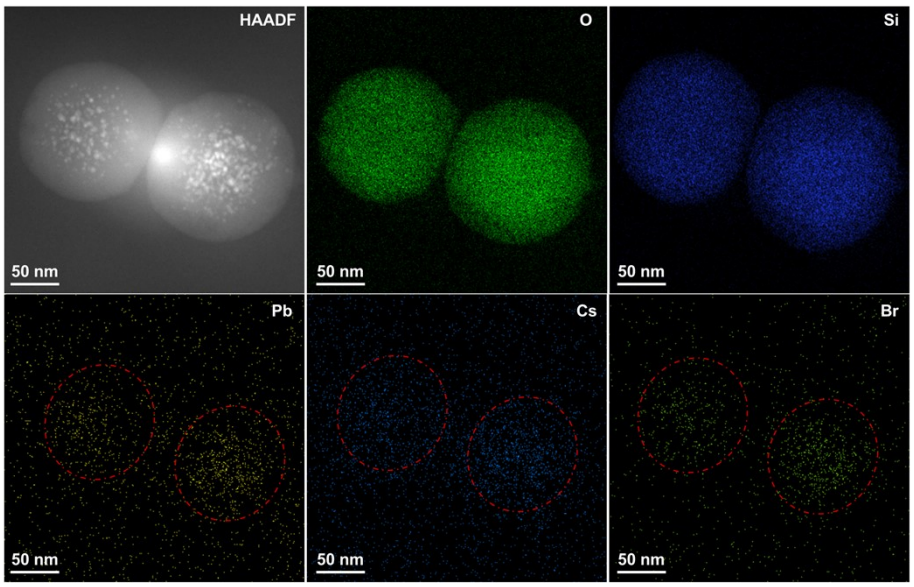

Figure S5. EDS mapping images of CPB@MSNs-3.17 nm, showing the element distribution of Si, O, Pb, Cs, Br.

Table S1. BET analysis of two as-prepared MSNs templates and resultant CPB@MSNs

Sample	Average pore size (nm)	BET surface area (m^2/g)	Volume of pores (cm^3/g)
MSNs-3.17 nm	~3.17	831.1	1.1456
MSNs-11.53 nm	~11.53	668.1	1.9023
CPB@MSNs-3.17 nm	~3.55	26.58	0.0621
CPB@MSNs-11.53 nm	~11.95	302.55	0.9966

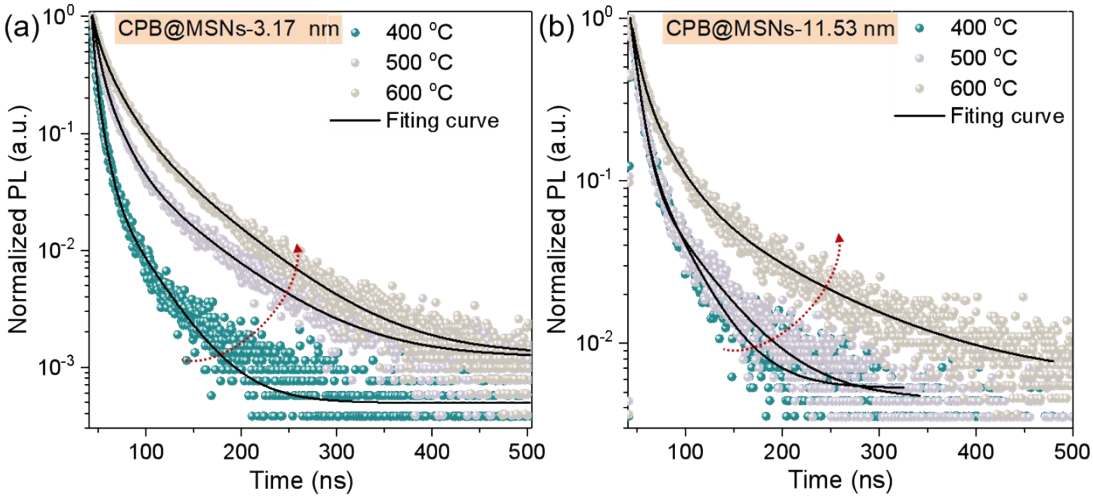

Figure S6. Time-resolved PL decay profiles of (a) CPB@MSNs-3.17 nm and (b) CPB@MSNs-11.53 nm at annealing temperature of 400 °C, 500 °C, and 600 °C.

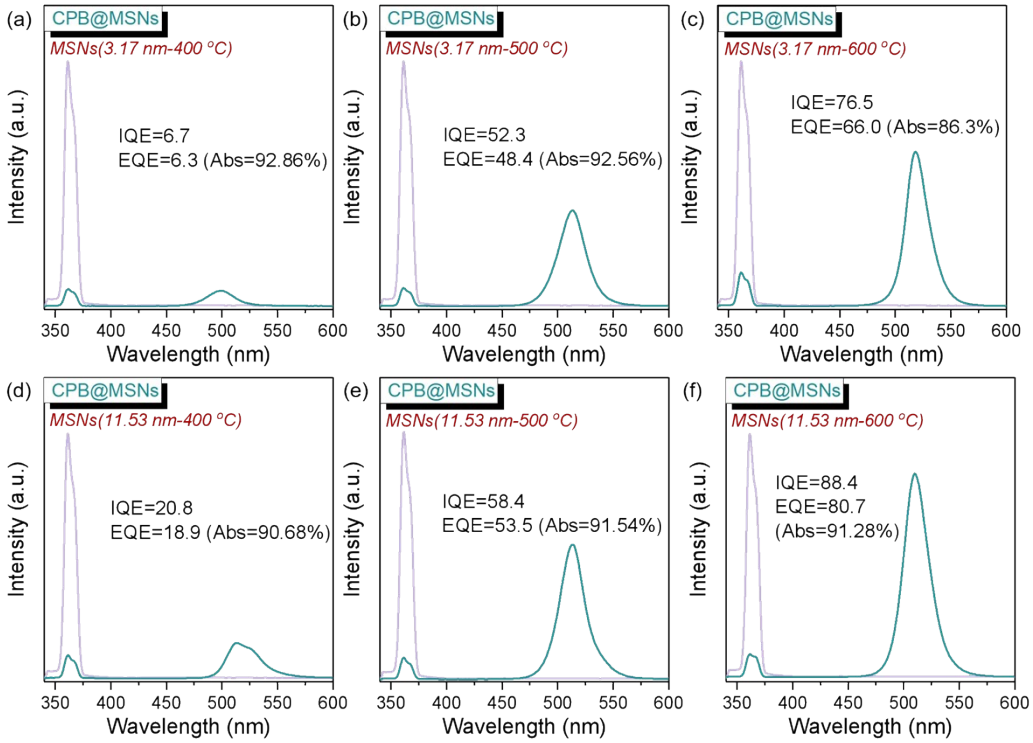

Figure S7. IQE and EQE measurements of CPB@MSNs (MSNs:3.17 nm, 11.53 nm; annealing temperature: 400 °C, 500 °C and 600 °C) powders.

Table S2. IQE, EQE, abs, and mean ± s.d. of the CPB@MSNs@Resin (pore size:3.17 nm; annealing temperature:500 °C)

Replicate	IQE(%)	A(%)	EQE(%)
1	71.5	89.0	63.6
2	72.4	89.2	64.6
3	73.3	89.4	65.5
mean ± s.d	72.4 ± 0.9	89.2 ± 0.2	64.6 ± 1.0

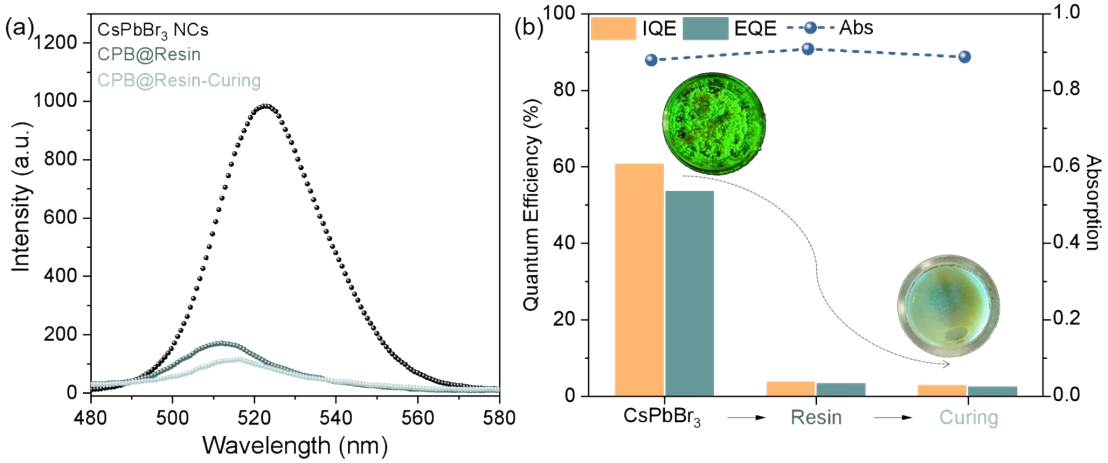

Figure S8. (a) Emission spectra and (b) IQE, EQE, and absorption of pristine $CsPbBr_3$ NCs, resin-encapsulated $CsPbBr_3$ NCs (CPB@Resin), and the cured composite (CPB@Resin-Curing). Inset in (b) shows fluorescence images of pristine $CsPbBr_3$ NCs and CPB@Resin-Curing under UV light excitation.

Figure S9. PLQY measurements of CPB@MSNs@Resin (MSNs:3.17 nm, 11.53 nm; annealing temperature: 400 °C, 500 °C, and 600 °C).

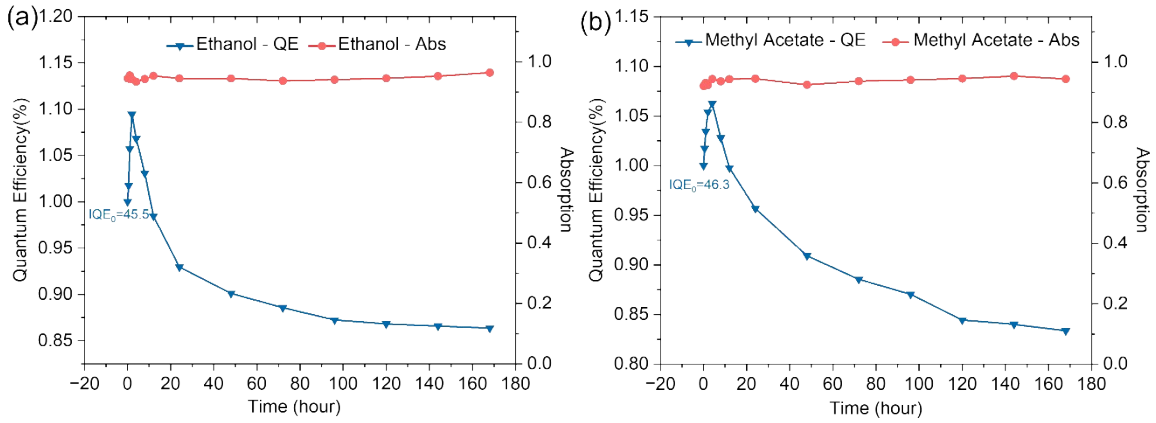

Figure S10. Absorption and IQE curves of CPB@MSNs immersed in (a) ethanol and (b) methyl acetate as a function of time (annealing temperature: 500 °C).

Table S3. Optical and Modeling Parameters Used in the Simulation

Parameter	Symbol / Setting	Value / Description
Refractive index of resin	n_resin	1.510
Refractive index of silica (SiO_2)	n_SiO_2	1.46
Effective refractive index of CPB@MSNs particles	n_CPB@MSNs	1.55 (effective medium approximation)
Effective refractive index of composite (4 wt% CPB@MSNs in resin)	n_composite	1.512
Absorption coefficient of resin at 405 nm	α_resin,405	0.0478 cm^{-1}
Absorption coefficient of composite at 405 nm	α_composite,405	7.78 cm^{-1}
Primary emission peak wavelength	λ	512 nm
Primary emission FWHM	FWHM	20.7 nm (502–522 nm)
Excitation / quantum yield model	/	Phosphor model driven by excitation spectrum (Fig. 1(e))
Particle geometry	/	Spherical
Particle size distribution (radius)	r	62.5–97.5 nm (centered at ~85 nm, unimodal)
Scattering model	/	Volumetric scattering based on Mie theory
Boundary conditions	/	Fresnel reflection at composite/air and composite/UV chip interfaces
Surface roughness	Ra	Neglected (Ra ≈ 0)

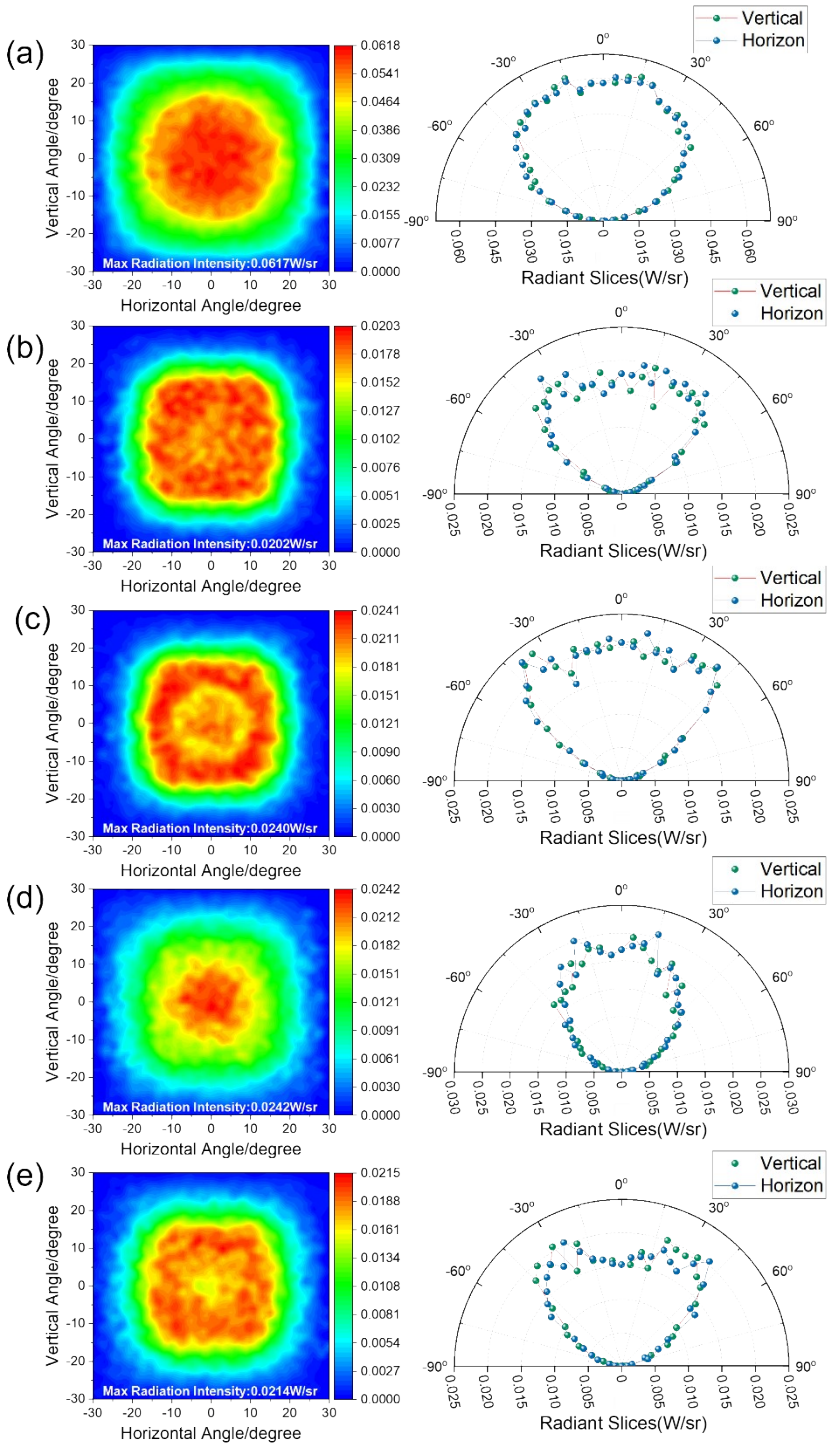

Figure S11. a (i)-e (i) Angular radiation intensity ($W \cdot sr^{-1}$) as a function of horizontal and vertical emission angles from the surface normal (a: planar film; b: hemisphere; c: truncated cone; d: inverted truncated cone; e: cylinder). Colors indicate decreasing intensity from red to blue. a (ii)-e (ii) Polar plots of the corresponding intensity profiles, with radial and angular coordinates representing radiation intensity and emission angle, respectively.